NASA/TM–2016-219364

Enabling Wireless Avionics Intra-Communications

Omar Torres, Truong Nguyen, and Anne Mackenzie
Langley Research Center, Hampton, Virginia

December 2016

NASA STI Program . . . in Profile

Since its founding, NASA has been dedicated to the advancement of aeronautics and space science. The NASA scientific and technical information (STI) program plays a key part in helping NASA maintain this important role.

The NASA STI program operates under the auspices of the Agency Chief Information Officer. It collects, organizes, provides for archiving, and disseminates NASA's STI. The NASA STI program provides access to the NTRS Registered and its public interface, the NASA Technical Reports Server, thus providing one of the largest collections of aeronautical and space science STI in the world. Results are published in both non-NASA channels and by NASA in the NASA STI Report Series, which includes the following report types:

- TECHNICAL PUBLICATION. Reports of completed research or a major significant phase of research that present the results of NASA Programs and include extensive data or theoretical analysis. Includes compilations of significant scientific and technical data and information deemed to be of continuing reference value. NASA counter-part of peer-reviewed formal professional papers but has less stringent limitations on manuscript length and extent of graphic presentations.

- TECHNICAL MEMORANDUM. Scientific and technical findings that are preliminary or of specialized interest, e.g., quick release reports, working papers, and bibliographies that contain minimal annotation. Does not contain extensive analysis.

- CONTRACTOR REPORT. Scientific and technical findings by NASA-sponsored contractors and grantees.

- CONFERENCE PUBLICATION. Collected papers from scientific and technical conferences, symposia, seminars, or other meetings sponsored or co-sponsored by NASA.

- SPECIAL PUBLICATION. Scientific, technical, or historical information from NASA programs, projects, and missions, often concerned with subjects having substantial public interest.

- TECHNICAL TRANSLATION. English-language translations of foreign scientific and technical material pertinent to NASA's mission.

Specialized services also include organizing and publishing research results, distributing specialized research announcements and feeds, providing information desk and personal search support, and enabling data exchange services.

For more information about the NASA STI program, see the following:

- Access the NASA STI program home page at http://www.sti.nasa.gov

- E-mail your question to help@sti.nasa.gov

- Phone the NASA STI Information Desk at 757-864-9658

- Write to:
  NASA STI Information Desk
  Mail Stop 148
  NASA Langley Research Center
  Hampton, VA 23681-2199

NASA/TM–2016-219364

Enabling Wireless Avionics Intra-Communications

Omar Torres, Truong Nguyen, and Anne Mackenzie
Langley Research Center, Hampton, Virginia

National Aeronautics and
Space Administration

Langley Research Center
Hampton, Virginia 23681-2199

December 2016

Available from:

NASA STI Program / Mail Stop 148
NASA Langley Research Center
Hampton, VA 23681-2199
Fax: 757-864-6500

1 Executive Summary

The Electromagnetics and Sensors Branch of NASA Langley Research Center (LaRC) is investigating the potential of an all-wireless aircraft as part of the ECON (Efficient Reconfigurable Cockpit Design and Fleet Operations using Software Intensive, Networked and Wireless Enabled Architecture) seedling proposal, which is funded by the Convergent Aeronautics Solutions (CAS) project, Transformative Aeronautics Concepts (TAC) program, and NASA Aeronautics Research Institute (NARI). The project consists of a brief effort carried out by a small team in the Electromagnetic Environment Effects (E^3) laboratory with the intention of exposing some of the challenges faced by a wireless communication system inside the reflective cavity of an aircraft and to explore potential solutions that take advantage of that environment for constructive gain. The research effort was named EWAIC for "Enabling Wireless Aircraft Intra-communications."

The E^3 laboratory is a research facility that includes three electromagnetic reverberation chambers and equipment that allow testing and generation of test data for the investigation of wireless systems in reflective environments. Using these chambers, the EWAIC team developed a set of tests and setups that allow the intentional variation of intensity of a multipath field to reproduce the environment of the various bays and cabins of large transport aircraft. This setup, in essence, simulates an aircraft environment that allows the investigation and testing of wireless communication protocols that can effectively be used as a tool to mitigate some of the risks inherent to an aircraft wireless system for critical functions.

In addition, the EWAIC team initiated the development of a computational modeling tool to illustrate the propagation of EM waves inside the reflective cabins and bays of aircraft and to obtain quantifiable information regarding the degradation of signals in aircraft subassemblies. The nose landing gear of a UAV CAD model was used to model the propagation of a system in a "deployed" configuration versus a "stowed" configuration. The differences in relative field strength provide valuable information about the distribution of the field that can be used to engineer RF links with optimal radiated power and antenna configuration that accomplish the intended system reliability. Such modeling will be necessary in subsequent studies for managing multipath propagation characteristics inside a main cabin and to understand more complex environments, such as the inside wings, landing gear bays, cargo bays, avionics bays, etc.

The results of the short research effort are described in the present document. The team puts forth a set of recommendations with the intention of informing the project and program leadership of the future work that, in the opinion of the EWAIC team, would assist the ECON team reach the intended goal of developing an all-wireless aircraft.

2 Background and Motivation

The Efficient Reconfigurable Cockpit Design and Fleet Operations using Software Intensive, Networked and Wireless Enabled Architecture (ECON) team is a world-class and interdisciplinary team working together to develop an ab initio prototype cockpit system. The design of the future cockpit system will be based on networked/cloud-architecture to support flight and fleet operations, wireless communications for control systems, and software-based cockpit interactions.

The goal of ECON will be met via three objectives: 1) increasing the use of software for operations and interactions, 2) implementing networked/cloud-based software systems to manage individual aircraft operations as well as entire fleets, and 3) increasing the use of wireless communication to channel the flow of information between intra-aircraft systems [1].

The increase use of wireless communication inside aircraft is a challenge that promises many improvements over the current fly-by-wire technology. Wireless systems would make it easier to access real time information in moving or rotating sub-systems where current wired architecture lacks continuous connections [2]. A perfect example of a gap in safety-related information is the lack of knowledge on the real-time conditions acting on a landing gear such as brake conditions, oleo pressure, and tire pressure [2]. The efficiency and reliability of an aircraft can be potentially enhanced by a wireless communication system that allows the flow of information to an automated system or pilot for real-time decisions and corrections.

A wireless system offers a dissimilar redundancy to wired connections and reduces the number of wires and connections that potentially break and cause failures and lengthy maintenance times. The reduction of wires in an aircraft include many potential improvements in safety, reliability, and operation and maintenance efficiency as well as environmental benefits associated with a reduction in the weight of the aircraft. Nevertheless, the implementation of a wireless system inside aircrafts is potentially more challenging than in other environments due to the reflecting nature of the airplane walls and bays that introduce multipath interference that affect the reliable flow of information. The communication environment is different in the different sections of an airplane: a passenger cabin with passengers, seats, and luggage is different than in the wings, tail and in the lower part of the airplane's compartment where mechanical and electrical/electronic systems come together is tight spaces.

As communication engineers explore wireless systems for intra-aircraft applications new solutions are sought in the open frequencies at 2.4GHz and 5.1GHz where there is ample inexpensive hardware availability and established protocols. However, the passenger demand for wireless connectivity during flight via Wi-Fi and Bluetooth technologies can make the wireless communication of aircraft systems even more challenging in these open frequency bands. An additional frequency band in the 4.2-4.4 GHz band has been requested by a group of researchers under the Aerospace Vehicle Systems Institute (AVSI) umbrella. This frequency band is currently allocated to the aeronautical radio navigation service (ARNS) for radio altimeters installed on board aircraft and for the associated transponders on the ground [3].

The wireless proliferation of passenger entertainment via personal and multimedia systems in addition to the proposed use of wireless methods of communications brings about a crucial importance to the understanding of the already dense electromagnetic environment inside an aircraft. Wireless communications for flight-critical and safety-critical functions require reliable flow of information that is guaranteed by several aspects of system design, one of which is the optimization of the EM/RF components, such as antennas, that function under the diverse environments present inside the different sections of the aircraft.

The EWAIC project summarized in this document takes advantage of the testing and modeling expertise and facilities existent in ESB to develop a capability to illustrate the complex electromagnetic environment inside aircraft and aid in the design of an aircraft communication system that includes flight and safety-related function

3 Enabling WAIC

The Enabling Wireless Aircraft Intra-Communication (EWAIC) project was formulated as part of the ECON seedling to provide the ECON project a means of incorporating basic electromagnetic theory into the engineering of an all wireless aircraft. The intended impact of EWAIC is to develop solutions that reduce the number of wire

harnesses inside aircraft and reduce the weight and complexity of critical systems that are necessary for reliable and safe flight. Using wireless systems for communicating critical system data is a promising solution.
At the fundamental level, electromagnetic fields provide the foundation of the digital protocols that exchange data wirelessly between two points, and understanding wireless systems at this level affords the advantage to engineer an EM link to maximize data exchange reliability. The metallic composition of aircraft structures are highly reflective to the radio signals of wireless communications systems and create an interference environment commonly known as multipath. The transmitted signals bounce off the reflecting surfaces in different directions and create patterns of interference that sometimes diffuse the direct line-of-sight communication and reduce the quality of the data link. Systems such as Wi-Fi, GPS, and others take multipath as a known problem and engineer a solution around it, but common applications for these systems usually involve entertainment and low-level navigation where signal dropouts do not endanger the user. Applications in which reliability is an utmost concern have the benefit of a thoroughly researched and understood operation environment that allows a well-engineered solution. For instance, GPS navigation in military aircraft employ highly engineered antennas, advanced signal processing, dual or triple frequencies, secretly coded signals, dissimilar systems, etc.

The EWAIC team expects the tight spaces of airplane compartments (e.g. avionics bays, landing gears, fuel tanks) to be detrimental to the quality of a wireless link for flight critical systems unless the multipath environment is considered during system design. For that purpose, EWAIC is taking the initial steps to develop a clear understanding of the EM environment inside aircraft. These steps consist of developing two methods of simulating the behavior of fields in the different compartments of an aircraft. One method is by creating a physical test environment where an airplane's multipath behavior can be replicated and serve as a test bed for digital communication systems. The second method consists of an initial computational modeling capability where the interference patterns of the different aircraft's subassemblies can be quantified and visualized to inform RF system design.

EWAIC was implemented using existing reverberating chamber facilities at NASA Langley Research Center as well as available EM computational modeling tools. The timeline of the project was such that it had to accommodate ongoing projects and was to be completed with limited resources to demonstrate potential capabilities instead of delivering full systems or solutions. The effort's duration was approximately three months and it included three RF engineers at a half time effort.

The objectives of the project were defined by the EWAIC team as:

1. To provide ECON a means of understanding the behavior of the multipath fields that envelop a wireless communication system and the understand system's performance inside aircraft
2. To demonstrate candidate tools and methods of RF engineering that may prove useful to a reliable wireless communication system

The approach implemented to reach the stated objectives was to conduct the two methods of investigation (computational modeling and physical test environment) as parallel paths that were complementary but independent of each other to maintain schedule. The task of linking the two methods to a point where the test environment validates and enhances the modeling component was left open for future efforts where resources would presumably allow it.

The final delivery would be in the form of a final report (presented herein) detailing the tools and methods developed to aid an all-wireless aircraft design.

The two methods are described in detail in the following sections.

3.1 Computational Modeling

3.1.1 Model description and setup

The computational EM model was set around a component area of an arbitrary airplane that was identified as a subsystem of interest by ECON [1] as well as AVSI [2]: the nose landing gear. The nose landing gear is a subsystem where available information is limited due to the lack of communication via networked architectures. Using wired connections on and around the rotating and moving parts of a landing gear represent an increased risk that make monitoring important parameters challenging. A wireless health monitoring system offers the potential of

informing pilots and other decision makers of the real-time conditions of the landing system, such as tire pressures and brake conditions, to enhance the operational efficiencies of the aircraft.

EM wave propagation in the vicinity of a nose landing gear also presents a challenging environment for wireless systems. This part of the aircraft is composed of mechanical parts of different materials and in complex shapes that are packed in tight compartments when stowed and deploy to open air when in use as the example shown in Figure 2. The EM environment varies from one of strong multipath conditions to one that may not be affected by multipath at all requiring the wireless link to function reliably in both environments.

To illustrate the difference in the interference pattern for both scenarios, a set of computer simulations were done using an available CAD model of a GMA-TT UAV, a scale model of a regional transport jet operated by the AirSTAR Program at NASA Langley (Figure 3). The simulations aimed to illustrate the field distribution of the two cases: one scenario that represents a deployed landing gear with no reflecting surfaces around the subsystem, and a second scenario where the system is enclosed by an all reflecting cavity, representing a stowed condition. Because the available UAV landing gear does not include a stowed position, a perfectly conductive cylinder was drawn around the CAD model to form an enclosure for the sake of simulating the stowing compartment. The two modeling scenarios are shown in Figure 4.

Simulations were carried out in two orthogonal planes, as shown in the right pane of Figure 4, with antennas in different locations on and around the landing gear. Two simple antennas were modeled; for some cases, a quarter-wave monopole was represented, while in other cases an ideal current source was used to simulate a short dipole.

It is understood that landing gears are different for different aircraft designs, and although the CAD model available to the EWAIC team did not correspond to a large transport aircraft, the simulation model itself was scaled so that the tires were 20 inches in diameter, which represents a size similar to a regional transport aircraft. For reference, regional jet nose wheel tires have the following diameters: Canadair CRJ-700, 20.5”; Embraer ERJ-135, 19.5”; Bombardier CL-600, 18.0”. The aircraft tires were assumed to be rubber with a relative permittivity of 3.2 – j0.02, while all other parts of the landing gear and its surrounding enclosure were assumed to be perfectly conductive.

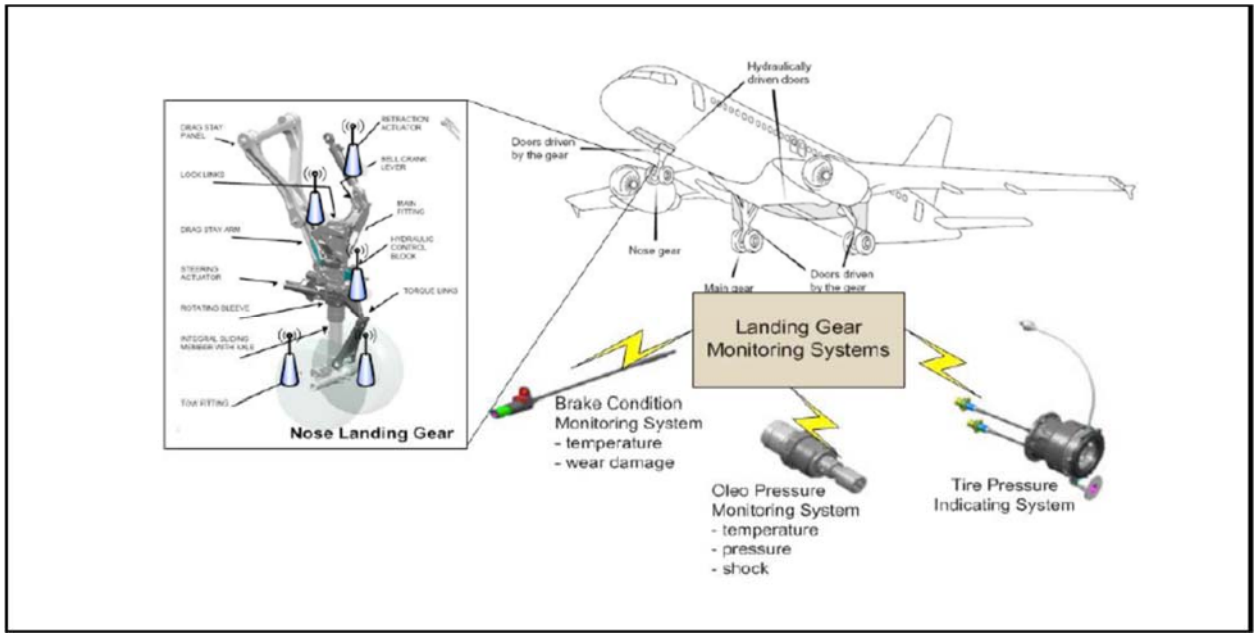

Figure 1. A wireless monitoring system on the landing gears provide information to the pilot or a flight computer to adjust flight operations according to the real-time conditions to improve system performance [2].

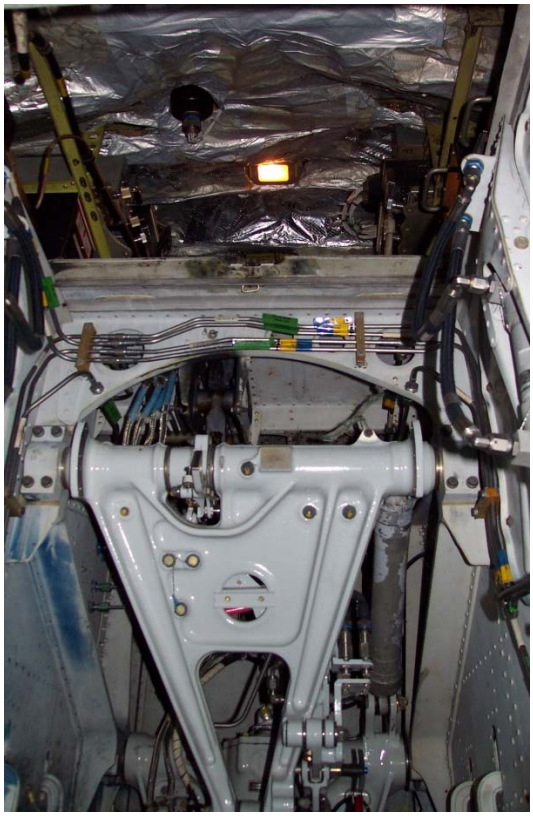

Figure 2. Nose landing gear of Embraer Jet aircraft

Figure 3. CAD model of the nose landing gear of the GMA-TT UAV used for the computational modeling task of EWAIC

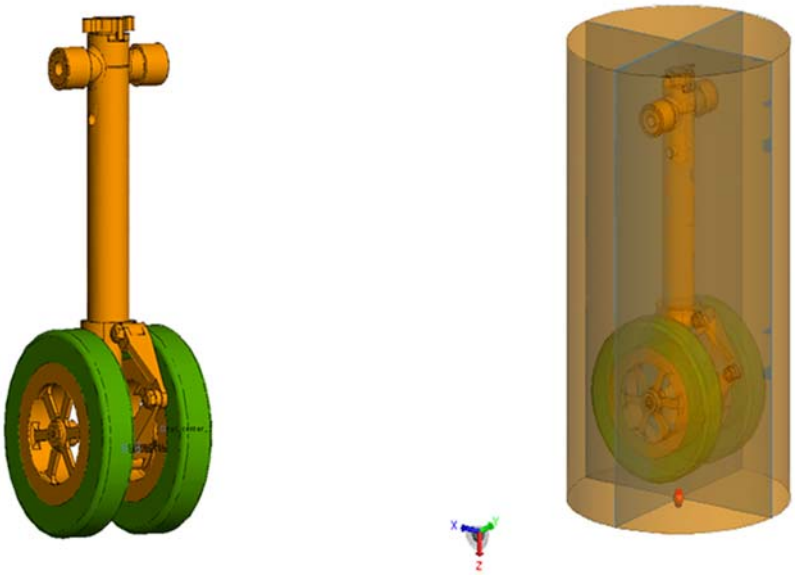

Figure 4. CAD model of the UAV nose landing gear in the deployed scenario (left) and inside the perfectly conducting cylinder depicting the stowed scenario (right). The figure on the right shows the two plane of study for each scenario

The computational modeling was done using the FEKO modeling software employing the multilevel fast multi-pole method (MLFMM). The MLFMM is a "fast" solver that allows the solution of electrically large problems on a workstation containing a moderate amount of RAM (64 GB). The nose gear-in-cylinder model was about 6.4 λ (wavelengths) in diameter and 11.6 λ in length at the chosen frequency of 2.4 GHz. Therefore, part of the modeled space was in the near field of a transmitting antenna, while part of the space was in the far field. This frequency was selected to coincide with the common communication protocols of interest in ECON: Wi-Fi and Bluetooth.

Several cases were modeled in each scenario to learn about the effects of interference relative to the location of the transmitting antenna. The antenna and the magnitude of the feed, either 1 V or 1 A, were chosen arbitrarily and are not fully representative of an operational system. In these cases, only the relative field strength distribution would be of importance. The modeled scenarios were as follows:

1. A vertical monopole antenna below the landing gear inside a conductive cylinder
2. A vertical monopole antenna above the landing gear inside a conductive cylinder
3. A horizontal monopole antenna next to the landing gear inside a conductive cylinder
4. Radiation Patterns inside the empty cylinder: monopole Vs. ideal current source antenna
5. Ideal current source antenna at lower end of cylinder
6. Ideal current source antenna at upper end of cylinder inside a conductive cylinder
7. Ideal current source antenna on strut lower surface in free space
8. Ideal current source antenna on strut lower surface in cylinder

3.1.2 Results and Analysis

Modeling results are displayed in 2-D plots representing cross sections of the cylinder in the X-Z and Y-Z planes with the landing gear strut being oriented along the Z-axis; all plots show the same points in space. Individual plots are labeled to show whether the plotted values represent total E-field magnitude, total H-field magnitude, or total Poynting vector magnitude. In this sense, total means inclusive of X, Y, and Z components. The color scales have been set to cover a -60 dB range from the highest value. On each plot, outlines of mechanical parts not in the plane of the plot are overlaid for reference.

The illustrations shown in Figure 5 show the result of illuminating the landing gear inside a conducting cylindrical enclosure with a Z-oriented monopole antenna as the source of illumination from below the landing gear. Portions of the landing gear that are metallic show no electric or magnetic fields inside their boundaries. The area of interest is in the space surrounding the landing gear and inside the cylinder walls because that is where information would presumably be communicated. Figures 5a and 5b show the E and H-fields in the orthogonal Y-Z plane. Electric

field strength is expressed as volts per meter, magnetic field strength in amperes per meter. Notably, in both views the H-field throughout the cylinder tends to be more homogeneous and brighter than the E-field, which varies by as much as 60dB. Patterns of repeated striation indicate the multipath effect.

Figure 6 shows the E and H-fields resulting from illuminating the landing gear inside a cylindrical enclosure using a Z-oriented monopole antenna placed above the landing gear. Again, there is significant blockage of the E-field, while the H-field appears to be more homogeneous and brighter.

Figure 7 shows the E and H-fields resulting from illuminating the landing gear inside a cylindrical enclosure using a Y-oriented monopole antenna placed to the side of the landing gear. Due to its placement, the antenna is obscured in the orientation depicted in the top two figures, but its location is shown in the bottom figures. The E and H-fields both show significant blockage by the landing gear.

Figure 8 is included to depict the radiation patterns of two different antenna types in the empty enclosure with only the cylinder walls to reflect energy. Both panes in the figure show the E-field magnitude in the X Z plane view; the left figure for a monopole antenna and the right figure for an ideal current source antenna. The ideal current source behaves as a small dipole and is a convenient feature included in the modeling software. The two antenna types in free space have very different characteristic patterns from each other; the in-cylinder patterns are also quite different from the free-space patterns. In free space, the E-field strength diminishes smoothly and continuously with distance away from the source. However, as seen in Figure 8, the effect of the closed container in both cases is to trap energy in the cylinder and distribute it so that the field strength is still high at the end distant from the antennas. A maximum path loss of 40-45dB is evident, whereas in free space the path loss would be more than 67dB. A striated pattern is visible in both plots due to the multipath effect of the enclosure, and energy is concentrated along the central long axis of the cylinder. It is not evident whether one antenna type or the other is preferable although they produce somewhat different patterns; various antennas such as these or patch antennas could be studied as potential candidates to a wireless communication system.

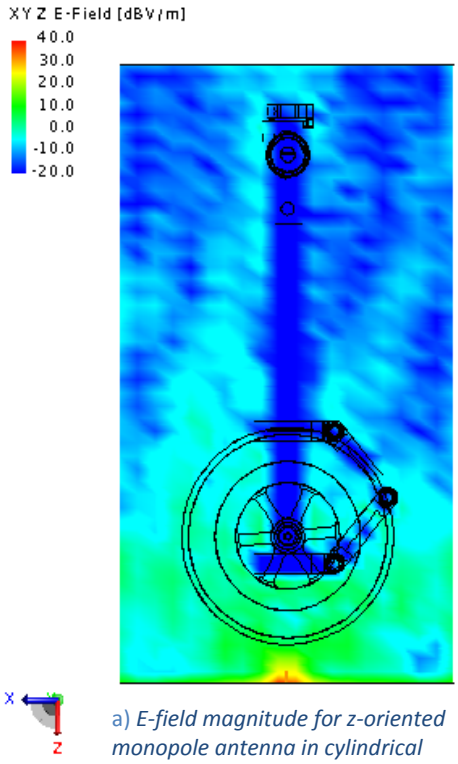

a) *E-field magnitude for z-oriented monopole antenna in cylindrical enclosure, X-Z plane*

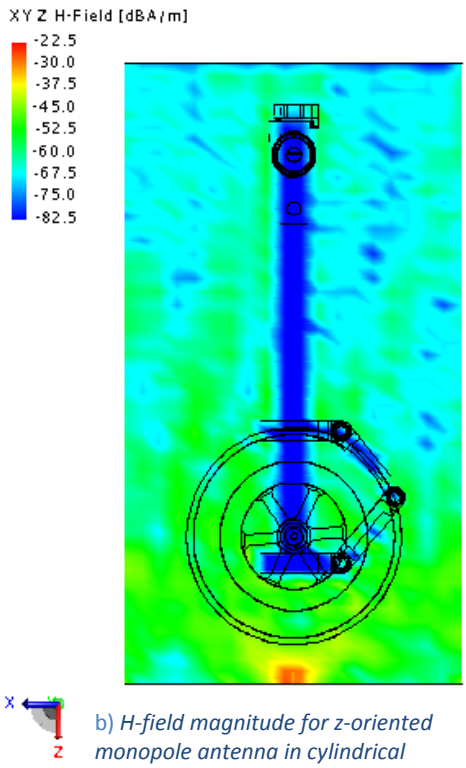

b) *H-field magnitude for z-oriented monopole antenna in cylindrical enclosure, X-Z plane*

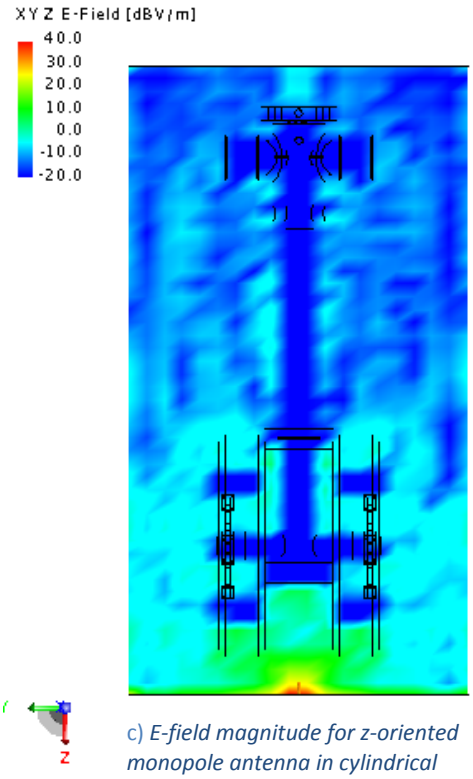

c) *E-field magnitude for z-oriented monopole antenna in cylindrical enclosure, Y-Z plane*

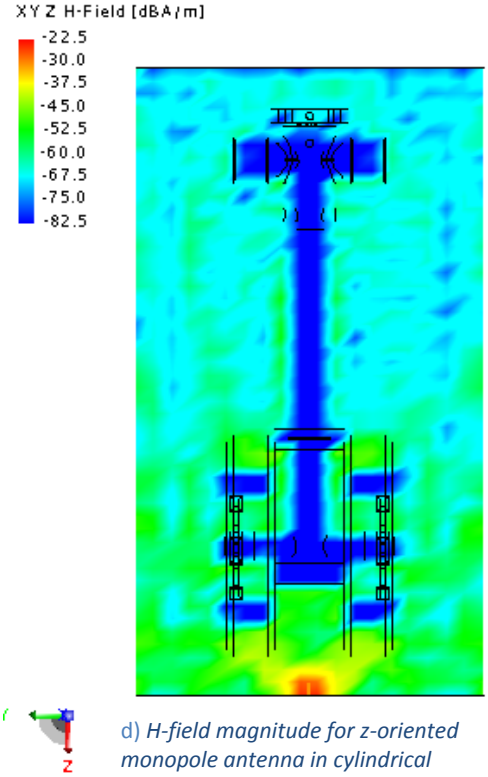

d) *H-field magnitude for z-oriented monopole antenna in cylindrical enclosure, Y-Z plane*

Figure 5. A vertical monopole antenna below the landing gear inside a conductive cylinder.

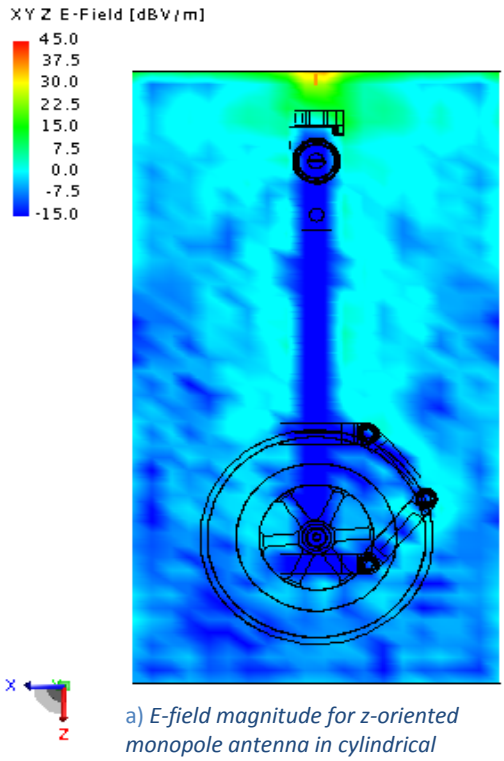

a) *E-field magnitude for z-oriented monopole antenna in cylindrical enclosure, X-Z plane*

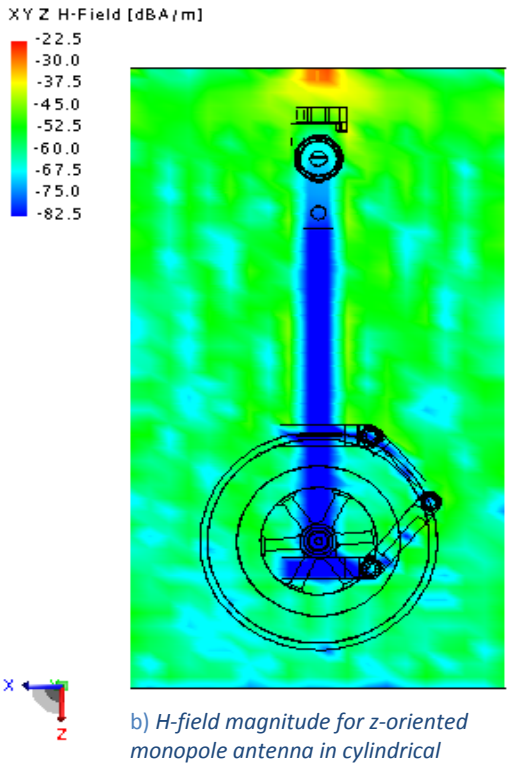

b) *H-field magnitude for z-oriented monopole antenna in cylindrical enclosure, X-Z plane*

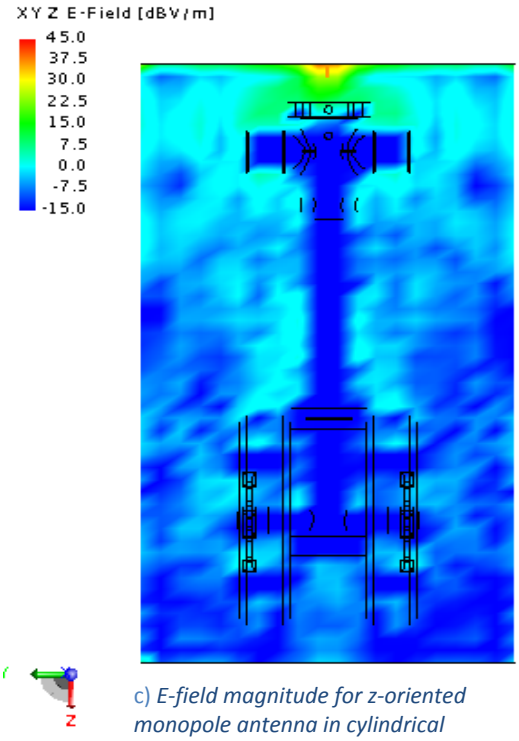

c) *E-field magnitude for z-oriented monopole antenna in cylindrical enclosure, Y-Z plane*

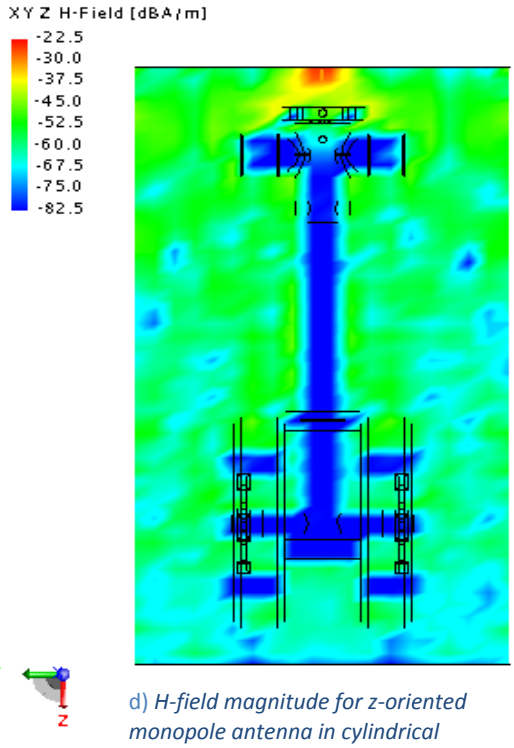

d) *H-field magnitude for z-oriented monopole antenna in cylindrical enclosure, Y-Z plane*

Figure 6. A vertical monopole antenna below the landing gear inside a conductive cylinder

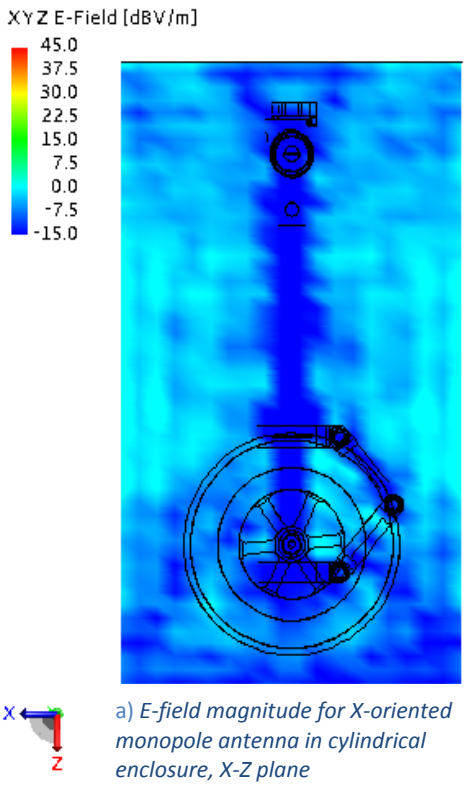

a) *E-field magnitude for X-oriented monopole antenna in cylindrical enclosure, X-Z plane*

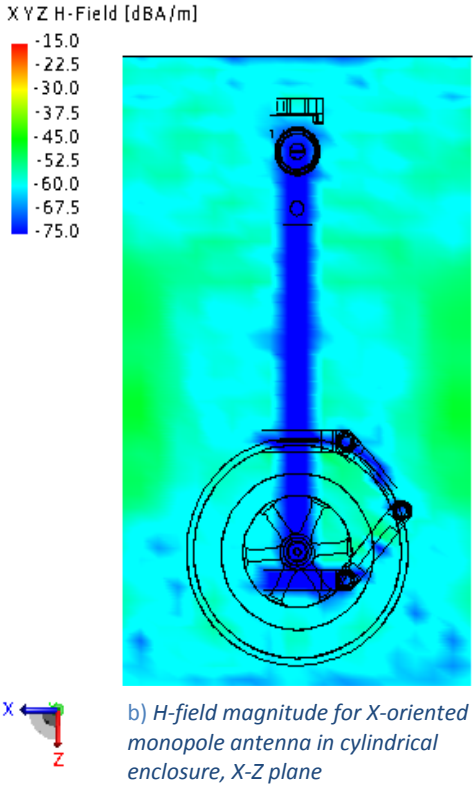

b) *H-field magnitude for X-oriented monopole antenna in cylindrical enclosure, X-Z plane*

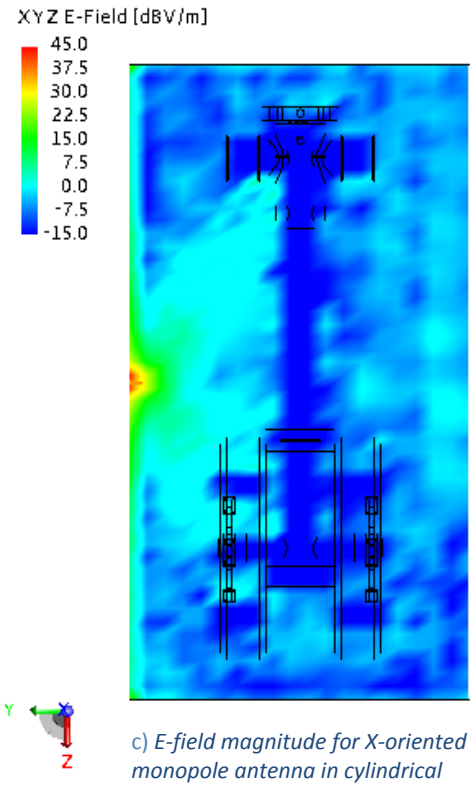

c) *E-field magnitude for X-oriented monopole antenna in cylindrical enclosure, Y-Z plane*

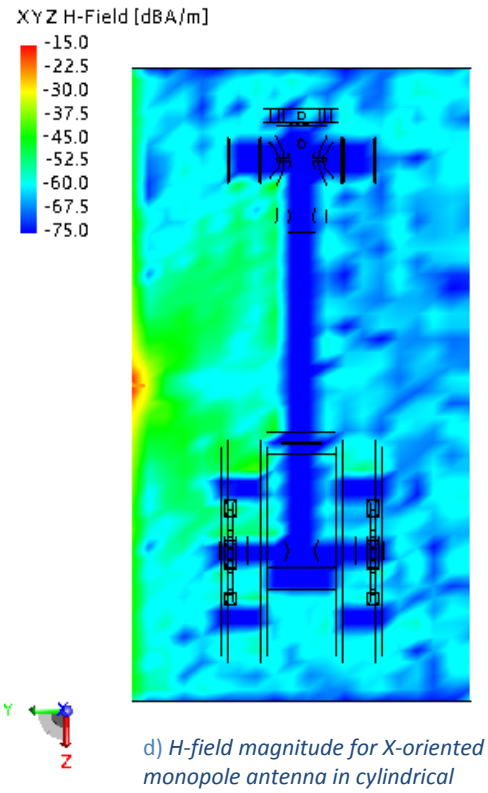

d) *H-field magnitude for X-oriented monopole antenna in cylindrical enclosure, Y-Z plane*

Figure 7. A vertical monopole antenna above the landing gear inside a conductive cylinder

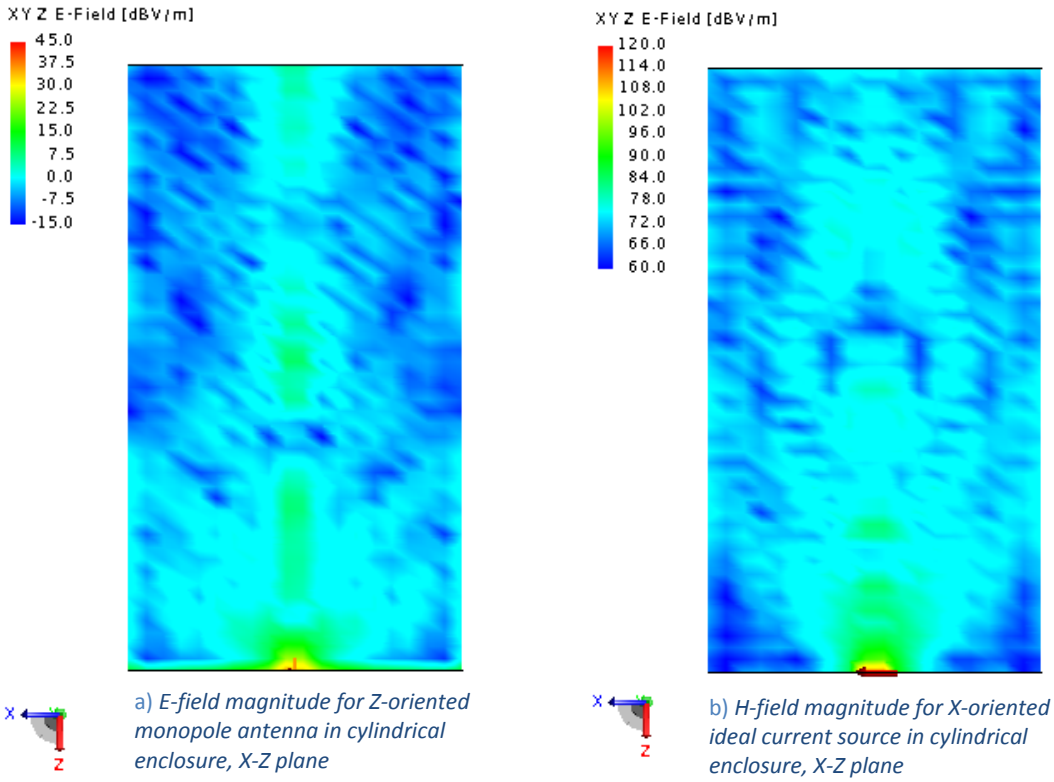

a) *E-field magnitude for Z-oriented monopole antenna in cylindrical enclosure, X-Z plane*

b) *H-field magnitude for X-oriented ideal current source in cylindrical enclosure, X-Z plane*

Figure 8. Radiation Patterns inside the empty cylinder: monopole vs. ideal current source antenna

Figures 9-12 show the total Poynting vector magnitude, which expresses the energy flux density contained in both the electric and magnetic fields. The Poynting vector (power density) units are watts per square meter. Figure 9 shows the Poynting vector magnitude for an ideal current source antenna located at the lower end of the cylinder. Similarly, Figure10 shows the Poynting vector magnitude for an ideal current source antenna located at the upper end of the cylinder. In these figures the difference in the radiated power is seen more clearly in the X-Z and Y-Z planes than those shown in the plots of the monopole antenna, which in free space would radiate equally in both planes. Overall, the power is less in the Y-Z plane compared to the X-Z plane. Multipath effects, that is irregular variation of power levels moving away from the antenna, are quite pronounced.

Figures 11 and 12 show the results for an ideal current source antenna attached directly to the lower end of the landing gear strut. Figure 11 shows the Poynting vector magnitude for the landing gear in free space, while Figure 12 shows the Poynting vector magnitude for the landing gear enclosed in a cylinder. In free space, metallic portions of the landing gear assembly block the radiated power in the upper vicinity of the nose landing gear. However, inside the cylinder, the cylinder walls redistribute the energy from the transmitting antenna so that the power is more homogenously distributed in the enclosure. Consideration for this effect must be made when designing the communication system for the landing gear either extended or retracted into a wheel well. Both in free space and in the cylinder, higher power levels are seen in the X-Z plane than in the Y-Z pane.

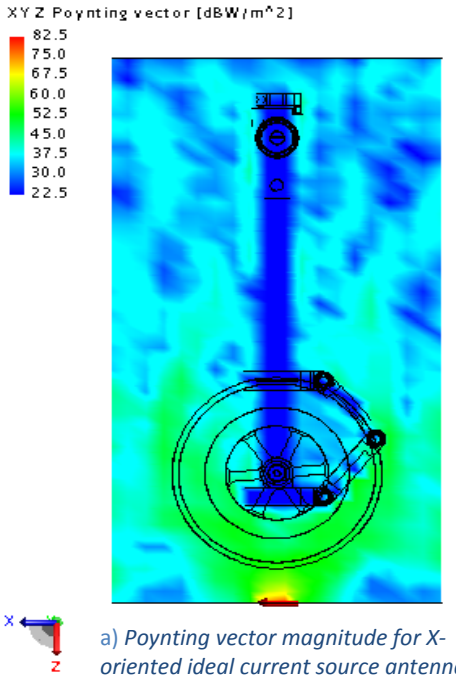

a) *Poynting vector magnitude for X-oriented ideal current source antenna in cylindrical enclosure, X-Z plane*

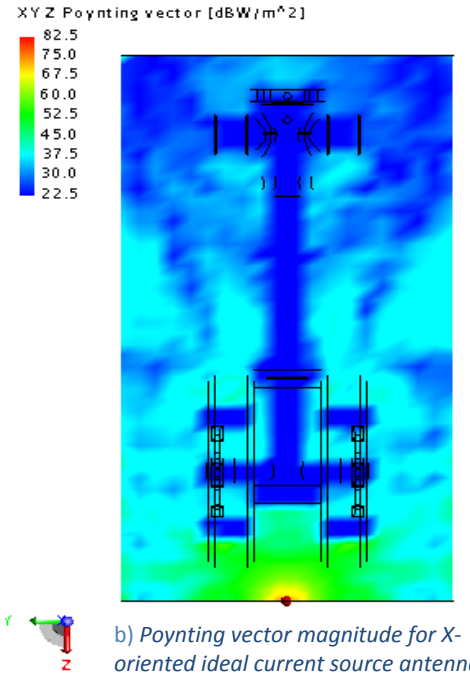

b) *Poynting vector magnitude for X-oriented ideal current source antenna in cylindrical enclosure, Y-Z plane*

Figure 9. Ideal current source antenna at lower end of cylinder

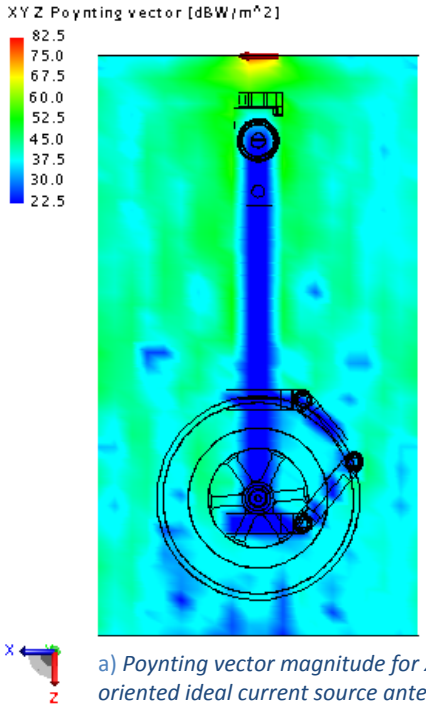

a) *Poynting vector magnitude for X-oriented ideal current source antenna in cylindrical enclosure, X-Z plane*

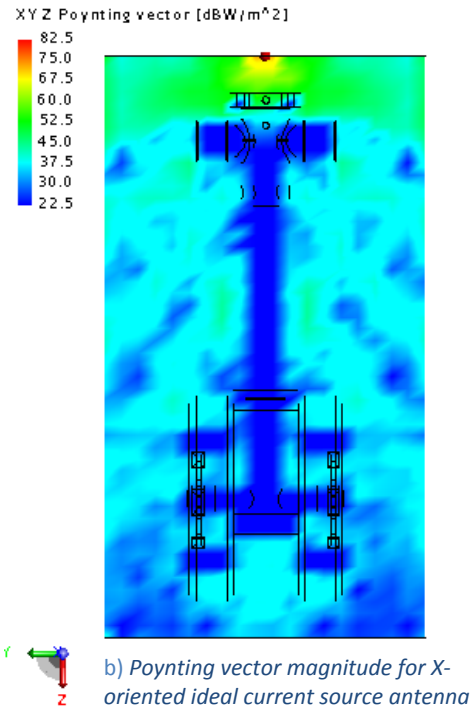

b) *Poynting vector magnitude for X-oriented ideal current source antenna in cylindrical enclosure, Y-Z plane*

Figure 10. Ideal current source antenna at upper end of cylinder

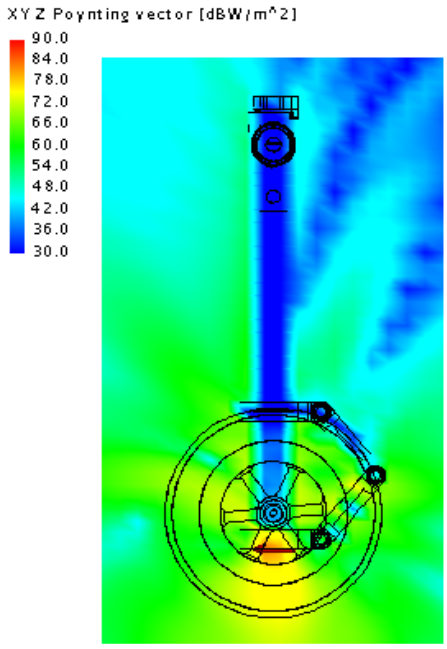

a) *Poynting vector magnitude for X-oriented ideal current source on strut lower surface in free space, X-Z plane*

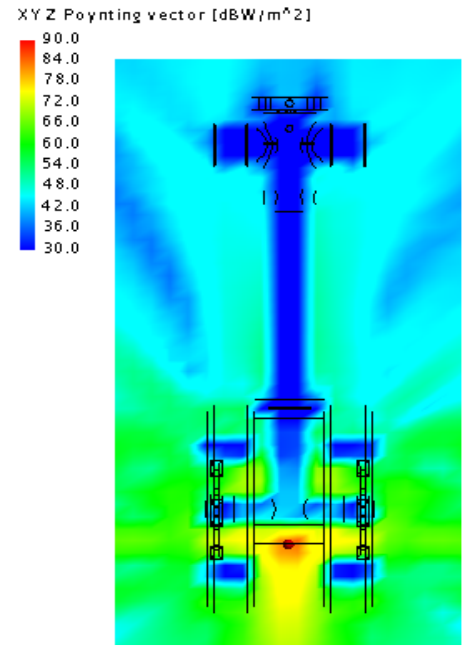

b) *Poynting vector magnitude for X-oriented ideal current source on strut lower surface in free space, Y-Z plane*

Figure 11. Ideal current source antenna on strut lower surface in free space

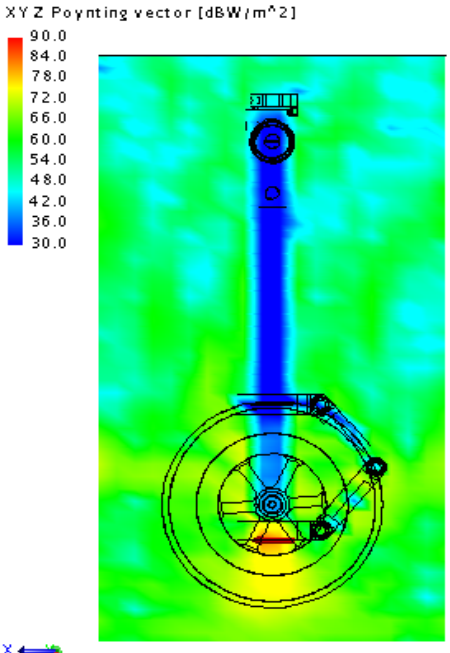

a) *Poynting vector magnitude for X-oriented ideal current source on strut lower surface in cylindrical enclosure, X-Z plane*

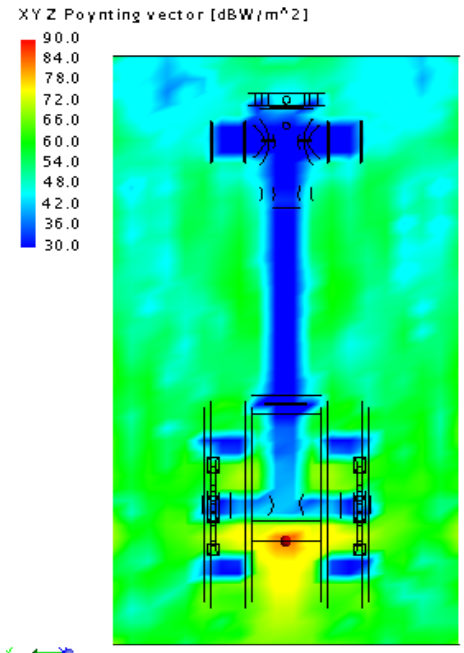

b) *Poynting vector magnitude for X-oriented ideal current source on strut lower surface in cylindrical enclosure, Y-Z plane*

Figure 12. Ideal current source antenna on strut lower surface in cylinder

3.2 Test Environment

3.2.1 Environment Setup

It has been shown in previous experiments and literature that the RF environment is different for the various cavities of an aircraft and that these environments can be replicated inside reverberation chambers [5]. A reverberation chamber is a highly conductive shielded room with one or more stirrers that mix EM radiated fields transmitted by an antenna within the chamber. Over many samples, the test field is isotropic, randomly polarized, uniform and statistically determined from the multi-mode complex fields.

Similar to internal aircraft environments, reverberation chambers are highly reflective to radio waves and cause wireless fading that results in poor communications or degraded data quality. The highly reflective environment exacerbates the fading effects and drowns out the more predictable line-of-sight components in mid to long ranges. Reverberation chambers are naturally suited for emulating aircraft wireless environments due to the similarity of the enclosed conductive walls. Using different antenna positioning, stirring techniques, and use of RF absorbing material, the chambers can also be used to emulate the Ricean fading of a possible aircraft wireless communications link where there exists direct line-of-sight (LOS) component in addition to the scattered field caused by multipath. For this project, a test setup was developed inside a reverberation chamber in the E^3 laboratory at NASA LaRC to mimic the environment inside an aircraft compartment and develop mitigation techniques for enhancing the reliability of a wireless communication link. The primary setup (Figure 13) consisted of a signal generator connected to a dual ridge horn antenna that enabled the transmission of RF signals inside the reflecting chamber. Three D-dot sensors were used as receive antennas each connected to a spectrum analyzer that captured and recorded the received power. The spectrum analyzers were synchronized via a function generator that simultaneously triggered the collection of power data from the three receiving antennas. In addition, an existing mechanical stirrer inside the chamber was operated at a rate of 2 revolutions/minute to produce reflections at different angles and induce a multipath effect with a statistically homogeneity that allows repeatability in testing. The primary test setup was devised to capture and study multipath data as well as to study a method of overcoming multipath interference by using antenna diversification. In addition, a secondary and similar test setup, shown in Figure 14, was formulated to study another mitigation technique based on the diversification of the frequency of the transmitted signal.

The center frequency chosen for the study of antenna diversification was 3 GHz. The intention of the team was to collect data near the 4.2-4.4 GHz frequency band, which is the target of the AVSI team for intra-aircraft wireless communication systems, but the hardware available for this study was limited in capacity to 3 GHz. For the frequency diversity study, two frequencies were used at 2.990 GHz and 3.000 GHz.
The chamber used for this test has a physical size of 47ft x23ft x9.5ft and a functional frequency range of 80 MHz – 18 GHz while maintaining up to 100 dB of shielding with the external environment. The instrumentation used for this experiment included those items in Table 1.

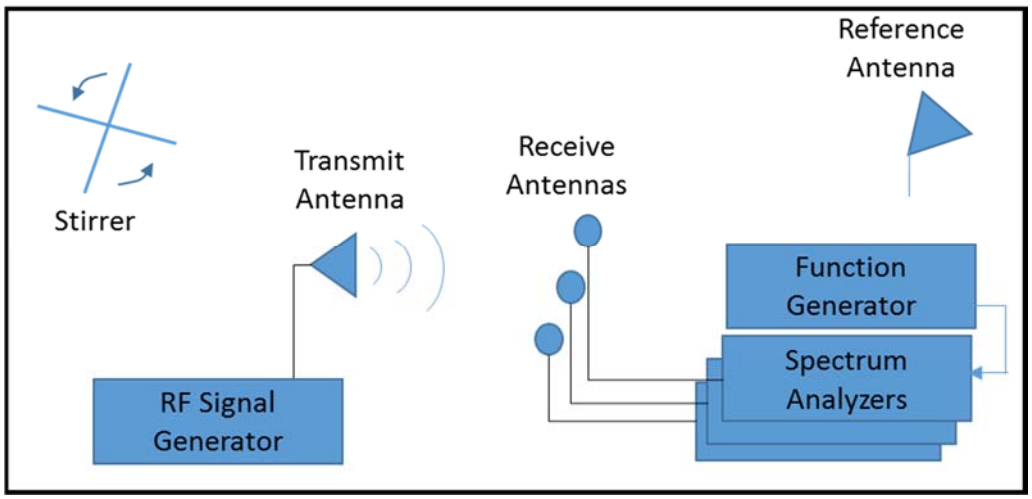

Figure 13. Test setup to study multipath effects with three receiving antennas at a single frequency

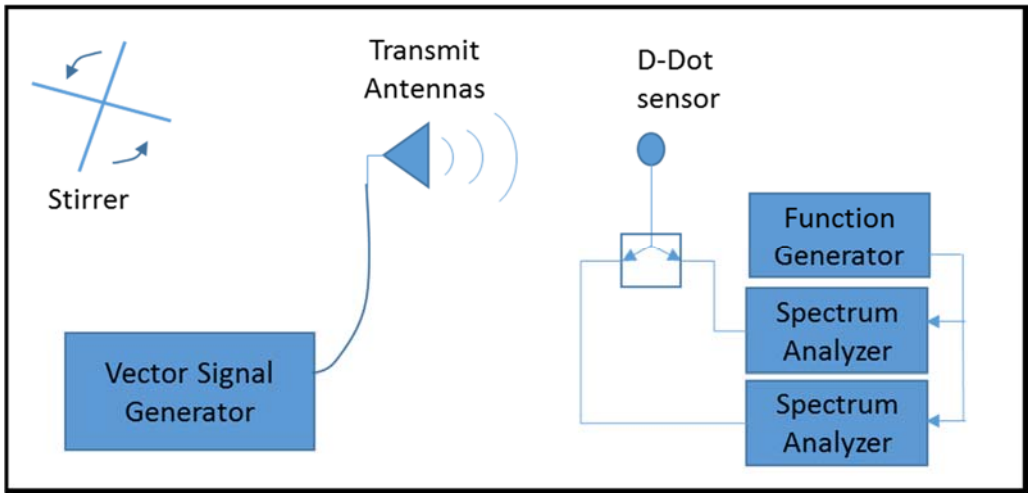

Figure 14. Test setup to study multipath effects with a single antenna at two different frequencies

Table 1. Instrumentation used for testing of multipath signals inside reverberation chamber

Manufacturer	Instrument	Model	# of units
Rohde & Schwarz	Vector signal analyzer	SMU 200A	1
Agilent	PSG Analog signal generator	E8257D	1
Agilent	Spectrum analyzer	E4402B	1
Agilent	Spectrum analyzer	E4407B	2
Agilent	Function generator	33220A	1
Prodyn technologies	D-dot sensor	AD-60C(A)	3
AH Systems	Dual Ridge Horn (DRG) antenna	SAS 200/571	2

3.2.2 Results and Analysis

The power collected with three D-dot sensors inside the reverberation chamber after two full revolutions of the stirrers (60 seconds) when using a 1mW (0 dBm) source is shown in Figure 15. The figure shows the power measured as the stirrers rotate and generate reflections in angles. The traces are instantaneously different, but over time the traces are statistically the same. The stochastic appearance of the power readings is mostly due to the interference pattern induced by the echoes inside the chamber. Some electronic noise in the hardware is part of the randomness, but this component is small relative to the intensity of the interference field present inside the chamber. A wireless communication system using a single antenna in this environment would be affected by the nulls observed in all three traces and would possibly manifest itself as data packets lost. The reliability of a safety-critical system with a single antenna in this environment would be questionable.

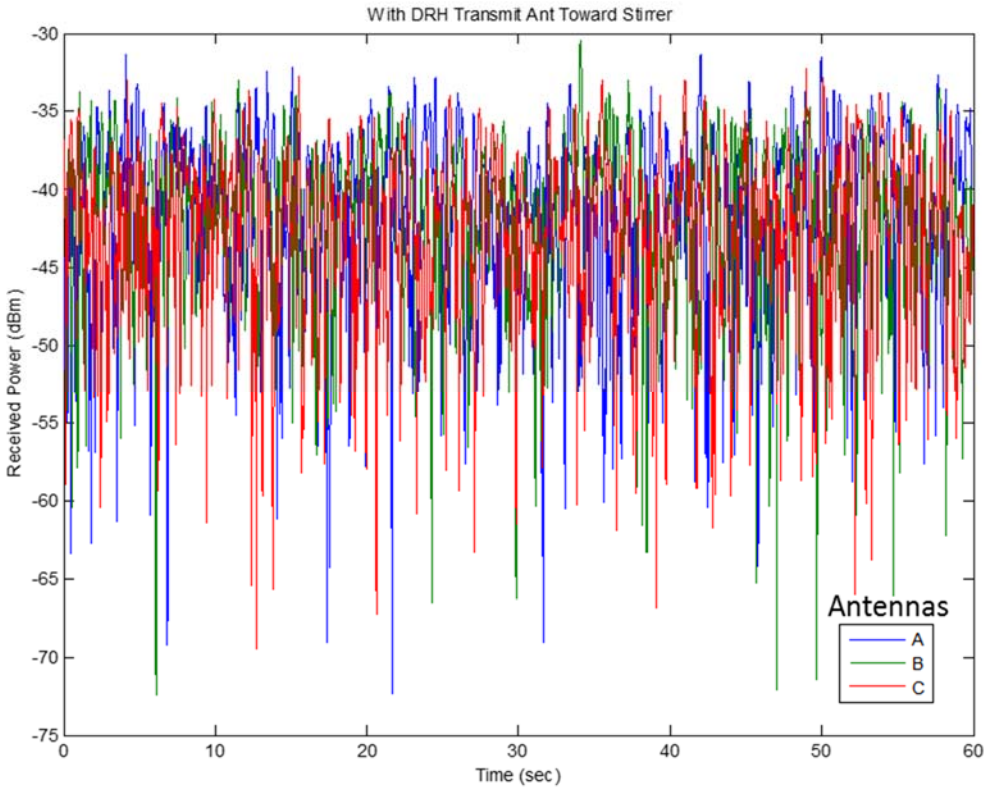

Figure 15. Power collected with three D-dot sensors inside a reverberation chamber

To minimize the occurrence of deep nulls, and increase the reliability of a communication system, a form of antenna diversity is implemented in which only the highest signal strength from the three D-dot sensors is used at any instant of time. This method takes advantage of the instantaneous disparity between the three traces and assumes that a null does not affect the three D-dot sensors at the same time. Figure 16 shows a traces composed of the highest instantaneous power between the three receiving antennas in use. This figure shows the dynamic range of the data in Figure 15 reduced significantly with the lowest signal approximately 20dB higher than the single antenna method.

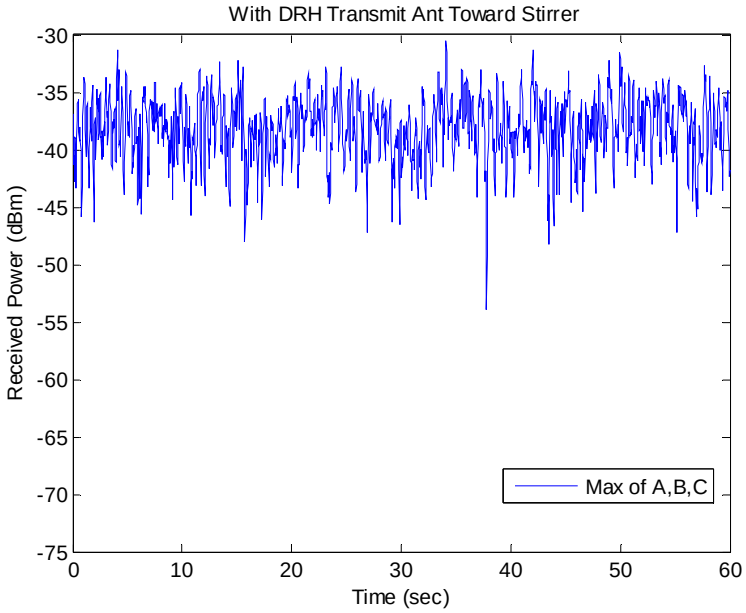

Figure 16. Highest instantaneous power observed between the three antennas used in the study

The quantification of the improvement in power level is shown by a cumulative distribution function in Figure 17 (in logarithmic scale) overlaid with the single antenna readings of Figure 15 labeled A, B, and C. The trace labeled "Max AB" is the highest power between traces A and B, and "Max ABC" is the maximum between the three antennas. This comparison shows that the diversification of received antennas results in a power gain of approximately 20dB for the three antenna case relative to the lowest power level observed by a single antenna. Also, it is shown that three antennas produce better results than two antennas. It is likely that more antennas produce better results, but the effect presumably reaches an asymptotical value and there is an expectation of a trade point where the improvement in power does not justify an increased number of antennas.

The benefits of the antenna diversity method are not as pronounced when there is a strong line-of-sight (LOS) component to the wireless communication system as shown in Figure 18. The figure shows the results of using three antennas inside the reverberation chamber with the transmit antenna pointing directly to the receive antennas from a distance of 0.5m. The traces in the CDF plot (right pane) shows that the maximum-level trace is not significantly better than the nearest single-antenna trace. This effect is explained by the overpowering of the LOS at this close distance where one of the antennas was thought to be within the main lobe of the antenna gain pattern. The LOS components are not the same for all three antennas due to the transmit antenna's beam width that was too narrow to completely cover the three receive antennas. The experiment was repeated at different distances with the results of 2 m and 5 m transmit antenna separation shown in Figure 18 and Figure 19 respectively. The figures show that the LOS component diminishes with distance and the fading component becomes more significant. It is evident that the choice of transmit antenna affects the results; the DRGhorn antenna used has a 10 dBi gain at 3 GHz. Other antennas with different gain patterns, such as an omni-directional antenna, would produce results where the fading components start to dominate at shorter distances.

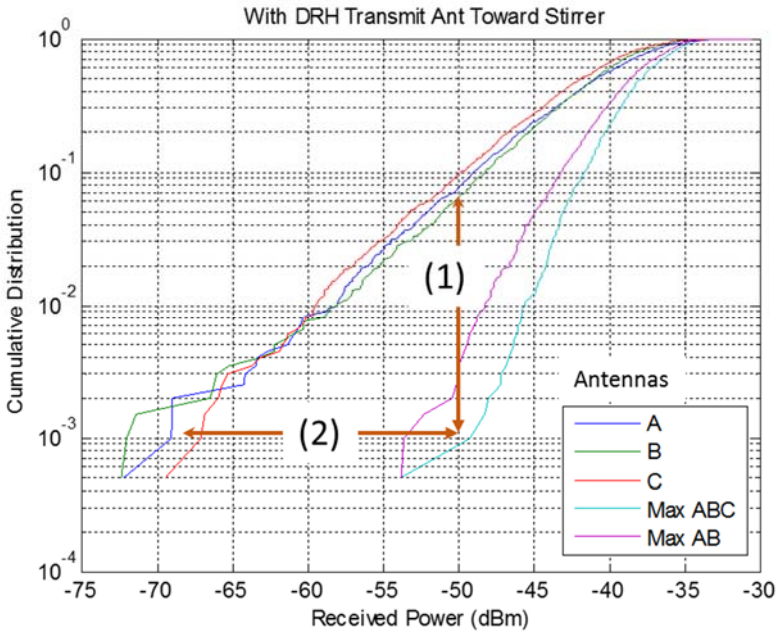

Figure 17. Quantified comparison of the effects of antenna diversity shows an improvement of up to 20dB at the lowest power level

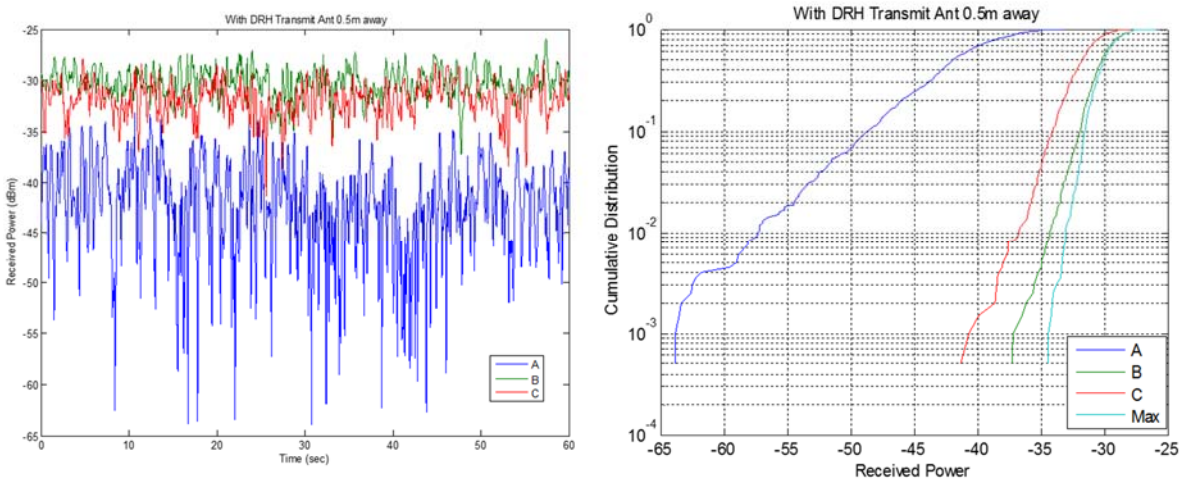

Figure 18. Power received by three antennas inside the reverberation chamber with the transmit antenna 0.5m away from the receive antennas

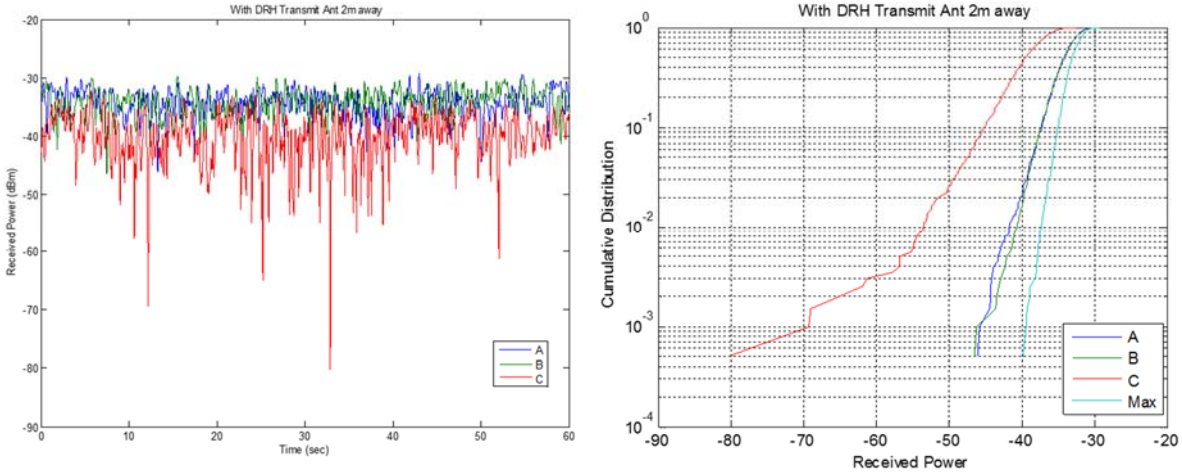

Figure 19. Power received by three antennas inside the reverberation chamber with the transmit antenna 2m away from the receive antennas

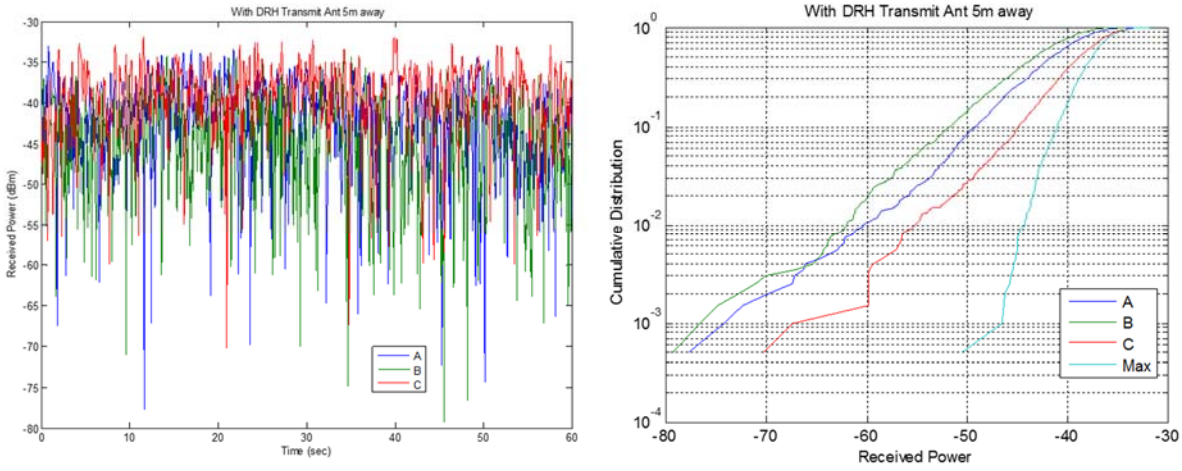

Figure 20. Power received by three antennas inside the reverberation chamber with the transmit antenna 5m away from the receive antennas

The LOS component produces a Rayleigh probability distribution with a non-zero mean similar to a Rice distribution that is measurable with laboratory equipment inside a reverberation chamber. These effects are shown in Figure 21 with the transmit antenna at different distances from the receive antenna. This figure illustrate effect of transmit-receive antenna separation in power; the intensity corresponds to the LOS component while the Rayleigh scattering around that intensity represents the multi-path component.

The effects of the LOS over that of the multipath interference effects can be quantified by using the Ricean K-factor, which is the ratio of the LOS power amplitude vs the multipath power amplitude. The average K-factors are shown in Table 2. The K-factor is shown to decrease with increasing distance between the two antennas. Ideally the multipath (non-LOS) K-factor should be close to zero.

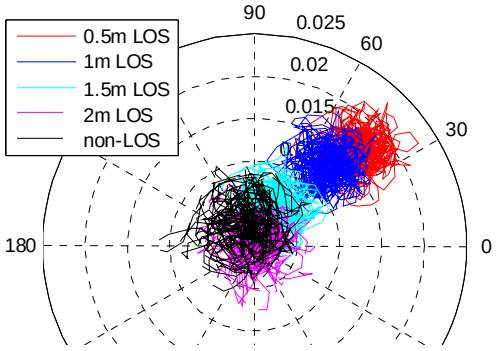

Figure 21. Amplitude of the LOS component with the transmit antenna at different distances from the receive antenna.

Table 2. Average K-factor of the power received by inside the reverberating chamber with varying separation between transmit and receive antenna and with the antennas pointing away from each other (non-LOS)

Distance	Average K-factor (dimensionless)
0.5m with LOS	30.2
1.0m with LOS	16.7
1.5m with LOS	4.59
2.0m with LOS	0.0197
Non-LOS 1	0.535
Non-LOS 2	0.362
Non-LOS 3	0.637

Changing antenna distance affect the LOS component, whereas reducing the reflecting capability of the chamber by adding signal attenuating material affects the fading component allowing both parameters to be adjusted to mimic those encountered in real aircraft cavities. The results presented by Hatfield et al in [5] demonstrate that reverberation chambers can be adjusted to mimic aircraft cavities. By introducing nine rectangular pieces of RF absorber of dimensions 16cm x 40.5cm x 182.5 cm to the NASA LaRC reverberation chamber the intensity of the multipath field was reduced up to 6dB, this demonstrating that the multipath environment of the Boeing 707 cockpit can be mimicked at 3GHz. The environment of the aircraft avionics bay was shown to be at lower levels of RF power, which means that this environment can also be simulated by simply introducing more absorbing material to the reverberation chamber. It is reasonable to expect that another 9 blocks of the same absorber would reduce the reflected signal power by the desired 12dB to mimic the RF environment of the avionics bays.

These measurements show that tuning cavity loss can be achieved in a reverberation chamber. It is unknown if wireless delay parameters can be matched for significantly different volumes (chamber vs avionics bay). If this were the case, smaller chambers could always be used to match the appropriate lag.

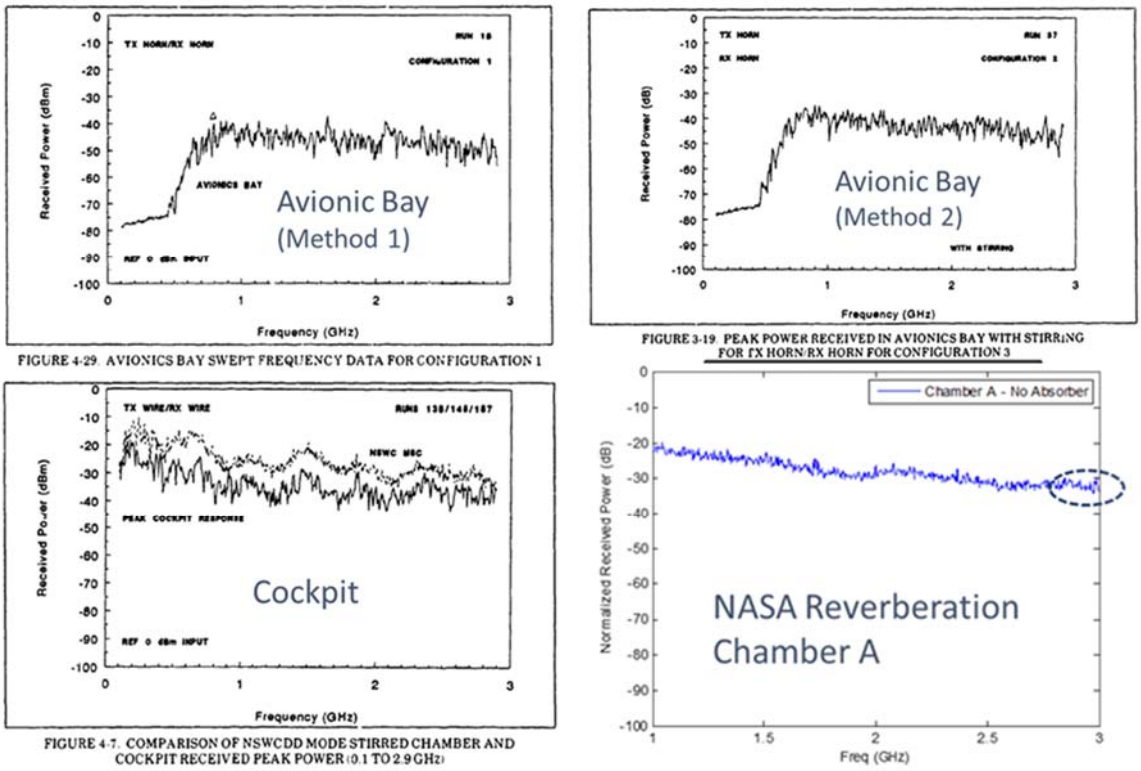

FIGURE 4-29. AVIONICS BAY SWEPT FREQUENCY DATA FOR CONFIGURATION 1

FIGURE 3-19 PEAK POWER RECEIVED IN AVIONICS BAY WITH STIRRING FOR TX HORN/RX HORN FOR CONFIGURATION 3

FIGURE 4-7. COMPARISON OF NSWCDD MODE STIRRED CHAMBER AND COCKPIT RECEIVED PEAK POWER (0.1 TO 2.9 GHz)

Figure 22. RF environment of different compartments in a Boeing 707 as demonstrated by Hatfield et al, and the environment in the NASA LaRC chamber with signal absorbing material (bottom right)

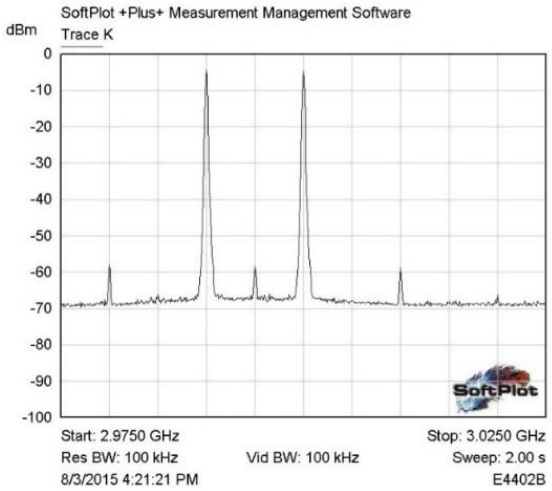

Figure 23. Two frequencies at 2.99GHz and 3.00 GHz (10MHz spectral separation) were used for the frequency diversity study

Figure 24. Test setup inside the reverberation chamber with the transmit antenna pointing directly at three D-dot sensors that acted as the receive antennas. All three receive antennas were used for the antenna diversity study while only one was used for the frequency diversity study

Similar to antenna diversity, using multiple frequencies and selecting the strongest signal could also provide power gain to help improve signal reliability. There are many approaches to achieving frequency diversity gain, including using multiple sets of transmit and receive antennas, or one transmit antenna with multiple receive antennas or vice versa; each transmit/receive antenna combination operate on a different frequency. These setups have the benefits of both antenna and frequency diversities combined. However, the setup used in this study uses only one transmit antenna and one receive antenna. This helps isolate the measurements to only frequency diversity with no effects from antenna diversity.

Multiple frequencies from the same transmit antenna are achieved by using a vector signal generator capable of multi-spectral output (up to 64 different frequencies in the specific instrument used). The number of frequencies dictate the number of spectrum analyzers used. In the example below, the vector signal generator produces two CW signals at 2.99 and 3.0 GHz (10 MHz spacing) as shown in Figure 18. Two spectrum analyzers are triggered by a function generator to simultaneously record the time traces of the power received at two separate frequencies. Figure 19 shows picture of the setup in the test chamber, with only the D-Dot receive antenna on the red stand being used for this measurement. The transmit antenna can be turned to direct away from the D-Dot receive antenna for minimizing the LOS component, or toward it if the presence of LOS component is desired.

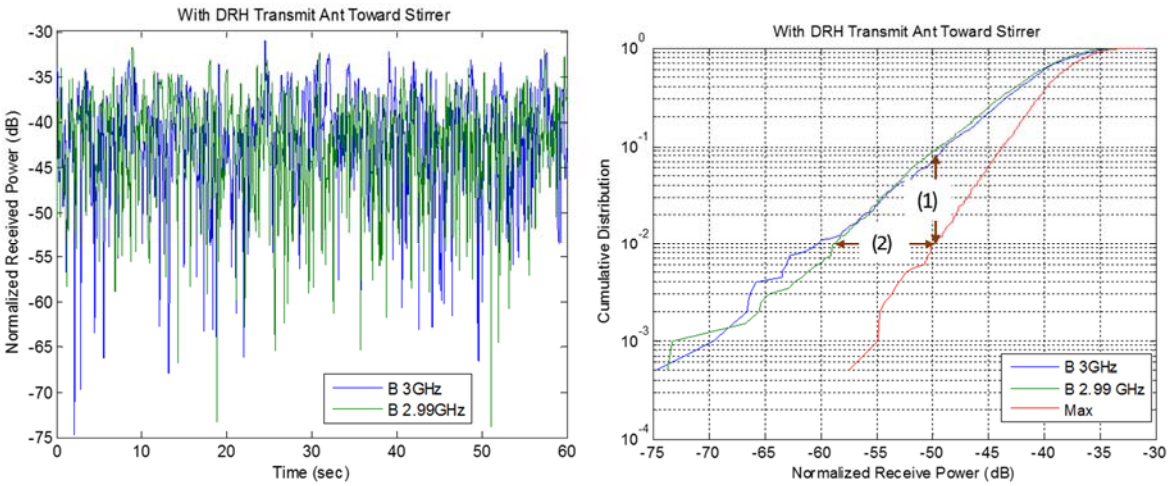

Figure 25. Power signals measured from the two frequencies. Frequency diversification show up to 20dB gain at the lowest power levels relative to a single frequency

Figure 25 illustrate the time traces measured by the two spectrum analyzers used in frequency diversity. Data are normalized to exclude cable loss and to have 0 dBm transmit power Comparing the cumulative distribution of the frequency diversity technique in Figure 25 against the results of antenna diversity shown in Figure 17, frequency diversity gain is almost as good as antenna diversity when using two antennas. At received power threshold of 50 dBm, frequency diversity improves the cumulative probability from about 10% to about 1%. At 1% cumulative probability, the receive power diversity gain is about 10 dB, denoted as (2) in the right pane of the figures. At the time of testing, a 3-way power divider was not available for measurements of three frequencies, thus only the two-frequency measurements are compared to the results obtained using two antenna diversification method.

Figures 26-28 illustrate the frequency diversity method when a LOS component is present with antenna separation of 1m, 2m and 5m. Even though the same antennas are used at the two close frequencies, the responses can be different even with a strong LOS component. The reasons for this characteristic behavior is not entirely clear, but it is possible that the behavior is induced by the antenna characteristics or by the phase different with the ground bounce between the two frequencies.

Comparing the two approaches, frequency diversity has the advantage of requiring less space – having one receive antenna versus multiple antennas – and can overcome RF interference at one of the frequencies. Antenna diversity, on the other hand, has redundant-antenna advantage and is more spectrum efficient. There may be other techniques to overcome multipath fading by increasing the LOS component, including using highly directional antenna or antenna with beam steering capability. In addition, optimizing the wideband digital modulation scheme or digital coding for the specific environment may provide additional tolerant to multipath fading. This could be a focus for future studies.

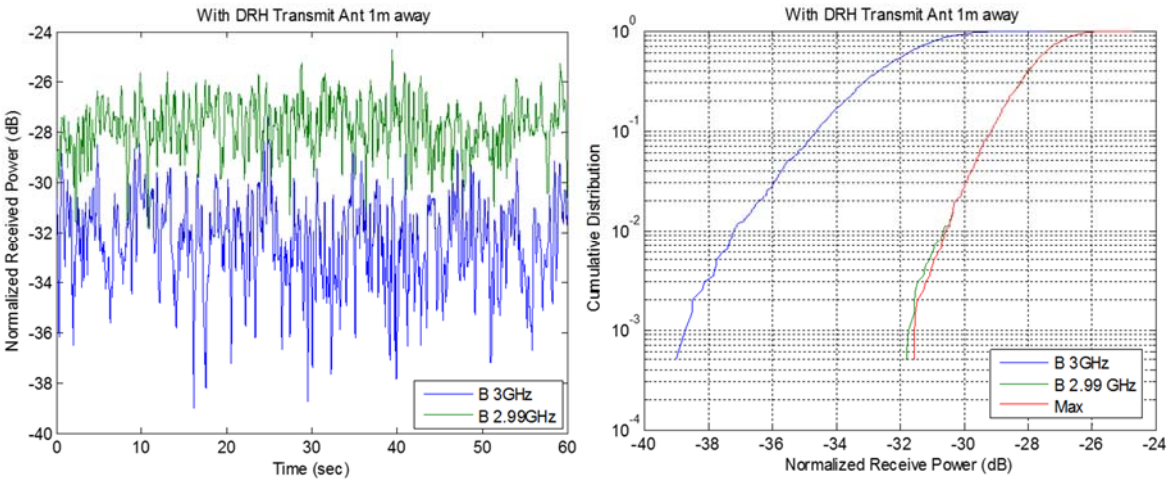

Figure 26. Frequency diversity measurement with a 1m antenna separation.

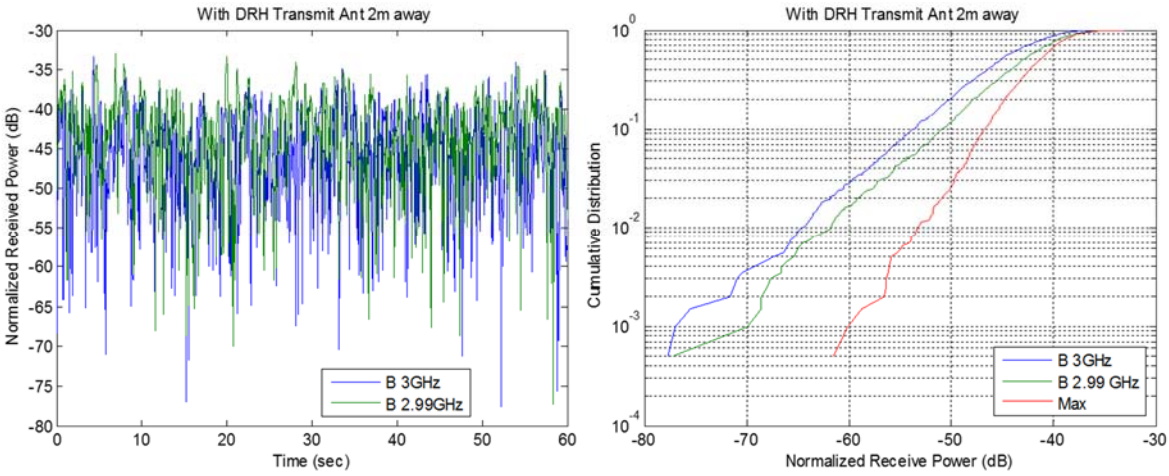

Figure 27. Frequency diversity measurement with a 2m antenna separation.

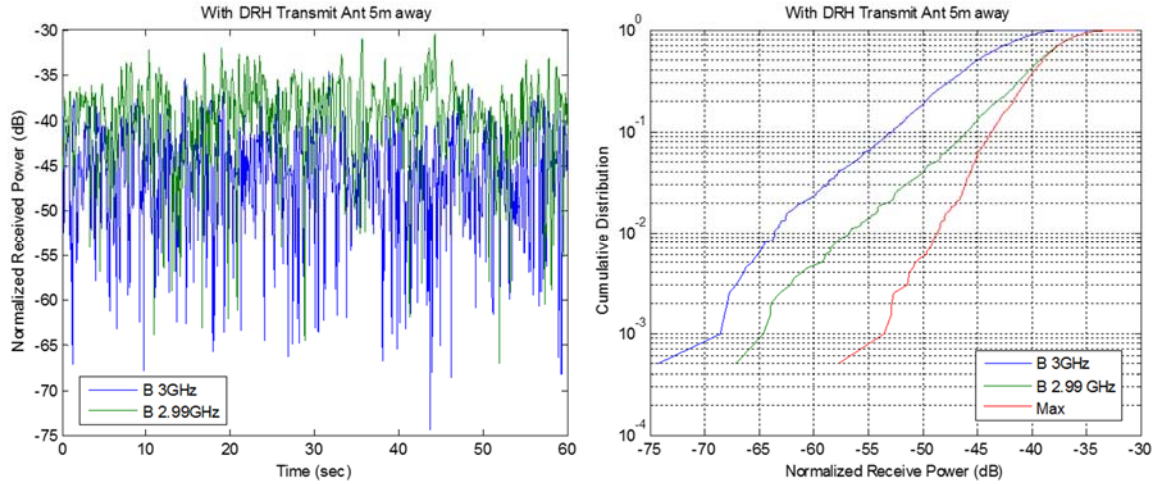

Figure 28. Frequency diversity measurement with a 5m antenna separation.

4 Recommendations for future work

1. Exercise the aircraft EM environment simulation method implemented in the reverberation chambers described in this report to develop and test the wireless communication protocols of the next generation aircraft as a cost saving alternative to testing in real aircraft.
2. Link the work performed as part of EWAIC to the efforts of the larger group called AVSI where the results of this work will benefit the conglomerate of industry, academia, and government who seek to implement wireless solutions on aircraft systems and bring efforts like EWAIC to the forefront of system development
3. Continue the development of the computational modeling tool described in this report to represent real transport aircraft and validate it using the chamber-based simulator to expand the quantification of the multipath environment inside the tight spaces of an aircraft assorted bays and cabins
4. Expand the knowledge database of the EM environment of aircraft beyond the 707 aircraft characterized in [5] to properly simulate the environments of different aircraft designs
5. Use of computational modeling tool to understand the fading of wireless signals and for modeling the full EM link from source to receiver for antenna design and placement to attain reliable flow of information

5 Conclusions

The EWAIC project demonstrates the use of a combination of computational modeling tools and RF measurement facilities can be used for the design and testing of the next generation aircraft wireless system. Using FEKO, the behavior of the electromagnetic field around an important aircraft subsystem was visualized to demonstrate the effects that the subsystem of an arbitrary aircraft has on the RF link of a wireless communication system. The electric field around a nose landing gear was shown to fade as much as 60dB when a transmit antenna was placed at the bottom of the landing gear. An enclosing reflecting cavity was used to induce multipath signals around the same nose landing gear as a "stowed" case. The enclosing cavity was shown to have some benefits when compared to the case where the subsystem was in the "deployed" case (in open air).

In addition, the EWAIC study demonstrates that reverberation chambers are good candidates for the simulation of aircraft RF environments. By adjusting the separation between antennas and introducing absorbing material to the chamber, both the line-of-sight (LOS) and the fading components of a wireless link inside the chamber can be adapted to test aircraft wireless communication systems in a relevant environment. The testing methods investigated include a form of antenna diversity as well as a form of frequency diversity. Gains of up to 20dB were estimated when using three receive antennas in a communications link that did not include a line-of-sight component. The results from the frequency diversity study showed similar results and demonstrated that either method is a viable solution inside a reverberating environment. A communication system with a line-of-sight component may not benefit from the diversity of antenna or frequency when the distance between transmit and receive antennas is short and the LOS component dominates the power spectrum. A wireless communication system with both LOS and fading components to its power spectrum was shown to have a Rice probability distribution.

This study illustrates measurements of modeling and testing several important wireless parameters using computational tools and existing reverberation chamber methods that could help design suitable wireless systems. Additional work is needed to develop this capability into an aircraft simulator, especially with the computational modeling tools where aircraft-specific components and volumes must be used to develop a well-grounded understanding of the behavior of the EM environment in real scenarios. In addition, digital communication protocols must be tested to understand how the error checking and error correction techniques of these protocols will work under the reverberating conditions in the allocated intra-aircraft frequency bands. The capabilities to develop a full aircraft simulation in a laboratory environment exist at NASA LaRC's research directorate.

6 Acknowledgments

The authors would like to thank Dr. Natalia Alexandrov of NASA LaRC for her advocacy and continued support that enabled this project. To George Szatkowski and Jay Ely for sharing their wisdom in technical matters, and to Brenda Kay for her invaluable help managing available resources.

7 References

[1] Efficient Reconfigurable Cockpit Design and Fleet Operations using Software Intensive, Networked and Wireless Enabled Architecture (ECON). Team seedling proposal submitted to NASA's Convergent Aeronautics Solutions project. Parimal Kopardekar, Principal Investigator.
[2] Aerospace Vehicle Systems Institute. http://avsi.aero/
[3] Report ITU-R M.2319-0. Compatibility analysis between wireless avionics intra-communication systems and systems in the existing services in the frequency band 4 200-4 400 MHz. November 2014
[4] Koppen, Sandra. A description of the software element of the NASA portable electronic device radiated emissions investigation
[5] M. Hatfield, G. Freyer, D. Johnson, and C. Farthing, "Electromagnetic Reverberation Characteristics of A Large Transport Aircraft," NSWCDD/TR-93/339, July 1994
[6] J. Ladbury, G. Koepke, and D. Camell, Evaluation of the NASA Langley Research Center mode-stirred chamber facility Nat. Inst. of Standards and Technology, Boulder, CO, 1999, NIST Tech. Note 1508

REPORT DOCUMENTATION PAGE

Form Approved
OMB No. 0704-0188

1. REPORT DATE *(DD-MM-YYYY)*
01- 12 - 2016

2. REPORT TYPE
Technical Memorandum

3. DATES COVERED *(From - To)*

4. TITLE AND SUBTITLE
Enabling Wireless Avionics Intra-Communications

5a. CONTRACT NUMBER

5b. GRANT NUMBER

5c. PROGRAM ELEMENT NUMBER

6. AUTHOR(S)
Torres, Omar; Nguyen, Truong; Mackenzie, Anne

5d. PROJECT NUMBER

5e. TASK NUMBER

5f. WORK UNIT NUMBER
533127.02.93.07.15.66

7. PERFORMING ORGANIZATION NAME(S) AND ADDRESS(ES)
NASA Langley Research Center
Hampton, VA 23681-2199

8. PERFORMING ORGANIZATION REPORT NUMBER
L-20720

9. SPONSORING/MONITORING AGENCY NAME(S) AND ADDRESS(ES)
National Aeronautics and Space Administration
Washington, DC 20546-0001

10. SPONSOR/MONITOR'S ACRONYM(S)
NASA

11. SPONSOR/MONITOR'S REPORT NUMBER(S)
NASA-TM-2016-219364

12. DISTRIBUTION/AVAILABILITY STATEMENT
Unclassified - Unlimited
Subject Category 01
Availability: NASA STI Program (757) 864-9658

13. SUPPLEMENTARY NOTES

14. ABSTRACT

The Electromagnetics and Sensors Branch of NASA Langley Research Center (LaRC) is investigating the potential of an all-wireless aircraft as part of the ECON (Efficient Reconfigurable Cockpit Design and Fleet Operations using Software Intensive, Networked and Wireless Enabled Architecture) seedling proposal, which is funded by the Convergent Aeronautics Solutions (CAS) project, Transformative Aeronautics Concepts (TAC) program, and NASA Aeronautics Research Institute (NARI). The project consists of a brief effort carried out by a small team in the Electromagnetic Environment Effects (E3) laboratory with the intention of exposing some of the challenges faced by a wireless communication system inside the reflective cavity of an aircraft and to explore potential solutions that take advantage of that environment for constructive gain. The research effort was named EWAIC for "Enabling Wireless Aircraft Intra-communications."

15. SUBJECT TERMS
Aircraft multipath; Reverberating chamber; Wireless avionics

16. SECURITY CLASSIFICATION OF:			17. LIMITATION OF ABSTRACT	18. NUMBER OF PAGES	19a. NAME OF RESPONSIBLE PERSON
a. REPORT	b. ABSTRACT	c. THIS PAGE			STI Help Desk (email: help@sti.nasa.gov)
U	U	U	UU	30	19b. TELEPHONE NUMBER *(Include area code)* (757) 864-9658